LBL-16789
UC-21 c.2

Lawrence Berkeley Laboratory
UNIVERSITY OF CALIFORNIA

Accelerator & Fusion Research Division

RECEIVED
LAWRENCE
BERKELEY LABORATORY

JAN 17 1984

LIBRARY AND
DOCUMENTS SECTION

HEAVY ION FUSION YEAR-END REPORT
April 1, 1983 - September 30, 1983

Heavy Ion Fusion Staff

November 1983

TWO-WEEK LOAN COPY

This is a Library Circulating Copy which may be borrowed for two weeks. For a personal retention copy, call Tech. Info. Division, Ext. 6782.

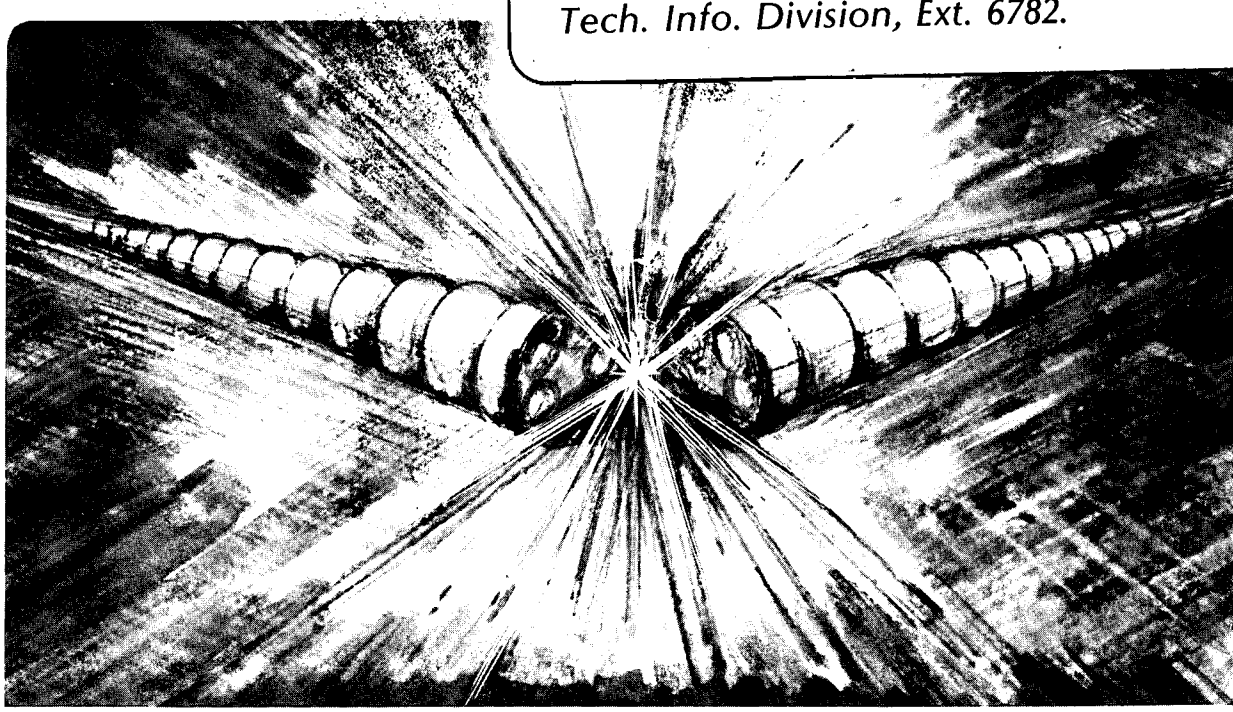

Prepared for the U.S. Department of Energy under Contract DE-AC03-76SF00098

LBL-16789 c.2

DISCLAIMER

This document was prepared as an account of work sponsored by the United States Government. While this document is believed to contain correct information, neither the United States Government nor any agency thereof, nor the Regents of the University of California, nor any of their employees, makes any warranty, express or implied, or assumes any legal responsibility for the accuracy, completeness, or usefulness of any information, apparatus, product, or process disclosed, or represents that its use would not infringe privately owned rights. Reference herein to any specific commercial product, process, or service by its trade name, trademark, manufacturer, or otherwise, does not necessarily constitute or imply its endorsement, recommendation, or favoring by the United States Government or any agency thereof, or the Regents of the University of California. The views and opinions of authors expressed herein do not necessarily state or reflect those of the United States Government or any agency thereof or the Regents of the University of California.

LBL-16789

HEAVY ION FUSION YEAR-END REPORT*

April 1, 1983 - September 30, 1983

Heavy Ion Fusion Staff

Accelerator and Fusion Research Division
Lawrence Berkeley Laboratory
University of California
Berkeley, California 94720

November 1983

*This work was supported by the Assistant Secretary for Defense Programs, Office of Inertial Fusion, Laser Fusion Division of the U.S. Department of Energy under Contract No. DE-AC03-76SF00098.

CONTENTS

	Page
HIGHLIGHTS	1
SINGLE BEAM TRANSPORT EXPERIMENT	2
Introduction	2
Experimental Results	2
Source Development	7
Faraday Cup Standards	8
Beam Attenuation and Emittance Control	8
BEAM DIAGNOSTICS DEVELOPMENT	10
Electron Beam Probe	10
Multiple Wire Beam Profile Measurements - "HARP"	10
NEUTRALIZED BEAM FOCUSING EXPERIMENT	13
MULTIPLE BEAM EXPERIMENT	17
INDUCTION ACCELERATOR DEVELOPMENT	18
Insulator Development	18
Long Pulse Induction Unit	23
THEORY	24
HTE Linac Design	24
HTE Final Transport	26
HTE Design - Final Focus	27
Spot Heating Calculations for HTE	31
Longitudinal Stability	34
Final Compression	35
Transverse Simulation	35

Page

PUBLICATIONS 37

H.I.F. STAFF ROSTER 38

DISTRIBUTION LIST 39

HIGHLIGHTS

- First results with the completed apparatus of the Single Beam Transport Experiment (SBTE) have shown the stable propagation of a space-charge-dominated cesium-ion beam through 41 periods of an AG focussing lattice. The space-charge effects were large enough to depress the betatron phase advance per cell from $\sigma_0 = 60^\circ$ to $\sigma = 12^\circ$. Thus, earlier conceptual designs for ion induction linacs, which assumed that a minimum σ-value was 24°, were probably too conservative.

- Understanding of the reflection stabilization of longitudinal instability in a high-current beam bunch has been improved by analytical and computational studies.

- Conceptual design studies of a multiple-beam ion induction linac suitable for the High Temperature Experiment have progressed to the stage where a first reference design (sodium, 125 MeV, 30 μC, 16 beams) is available. While probably far from an optimum, the example design serves as a guide in identifying certain physics and engineering problems that must be addressed in the R and D program.

- The Long-Pulse Induction Accelerating Unit, first used to accelerate a cesium-ion beam in February 1983, has been undergoing modification in the low-level trigger circuitry to allow more precisely controlled waveform synthesis.

SINGLE BEAM TRANSPORT EXPERIMENT

Introduction

The Single Beam Transport Experiment is intended to investigate the long-term stability of heavily space-charge loaded ion beam transport in an alternating gradient lattice, with the goal of characterizing stability thresholds and instability modes. The threshold information is of immediate interest in the optimization of the accelerator design for the proposed High Temperature Experiment, as well as for longer term heavy ion beam-driven fusion development. The relevant parameters are the single particle phase advance per focusing period (σ_0) and the space-charge reduced phase advance (σ). As current density increases, σ falls toward zero. However, there is no experimental knowledge of whether $\sigma \rightarrow 0$ can be physically realized, or if collective effects cause degradation of beam quality at some lower current density.

As of March, 1983, we had in operation a source of Cs^+ ions, five quadrupoles individually powered to match the axi-symmetric beam from the source into the alternating gradient transport lattice, and ten quadrupoles of that lattice in place. We had begun measurements with approximately matched beam parameters for a wide range of σ_0 values at a fixed normalized emittance of $.8 \times 10^{-7}$ π meter radians. Early results were reported at the IEEE Particle Accelerator Conference in Santa Fe.

Experimental Results

During this reporting period we have added quadrupoles Q-11 through Q-82, making available the full 42 lattice periods of transport over a distance of 13 meters, and have begun precise matching procedures and beam

characterization. (See Fig. 1.) We have also installed various diagnostics to be described below, including a deep, gridless Faraday cup and a biased set of grids to increase the beam emittance in a controlled way.

While we intend to carry out an extended program of measurements of beam behavior in a long AG transport channel as a function of current (I), phase advance (σ_0), and emittance (ϵ_N), we concentrated first on identifying at least some favorable conditions for transporting high currents. Such results have a direct and immediate impact on the design assumption on permissible tune depression (σ/σ_0) being used in the design of the High Temperature Experiment (HTE). Guided by theoretical and simulation predictions, we concentrated our first efforts on exploring values of σ_0 in the neighborhood of 60°. A first encouraging result was that the full beam current (11 mA) was seen to be transmitted without attenuation through the 82-quadrupole transport lattice for $\sigma_0 = 45°$, 60°, and 90°, the beam matching being appropriately adjusted for each case.

The most extensive measurements were made for $\sigma_0 = 60°$, for three values of beam current (1.3 mA, 6 mA, and 11 mA), and two values of emittance ($\epsilon_N = 1.2$ and 5.0×10^{-7} rad-m). The experimental procedure consists in adjusting the matching quadrupoles M1-M5 to obtain a matched beam in the transport line Q1-Q82, and then measuring the current, emittance, and size of the matched beam at Q82. It is important also to verify that the beam current, emittance, and size at the exit of Q82 are the same as the values entering Q1. By using the KV envelope computer codes the value of the depressed phase-advance, σ, can be inferred from a measurement of ϵ_N together with a measurement of <u>either</u> the beam current or the beam size. The six data points plotted in Fig. 2 show consistency between both methods of deriving the depressed tune and correspond to $\sigma = 57°$, 45°, and 36° for

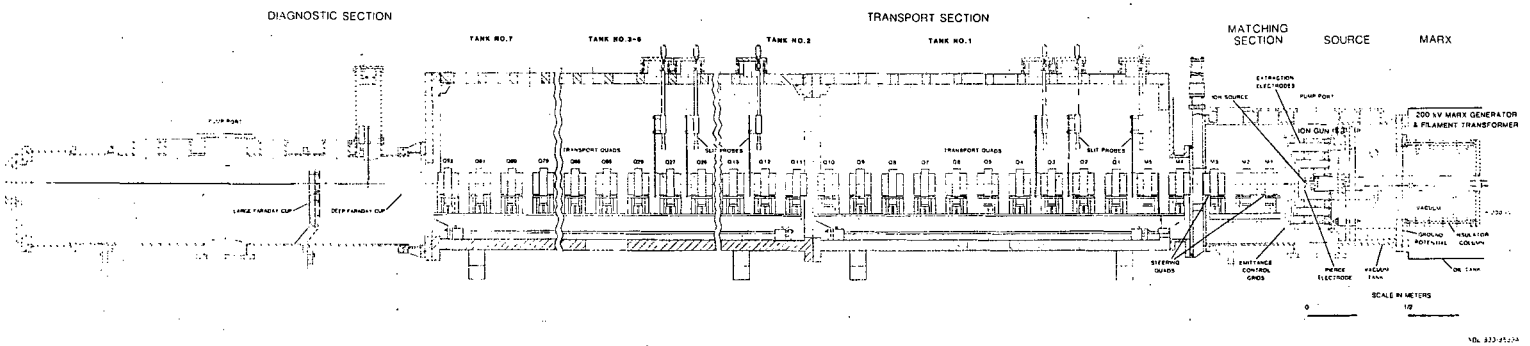

SINGLE BEAM TRANSPORT EXPERIMENT

FIG. 1

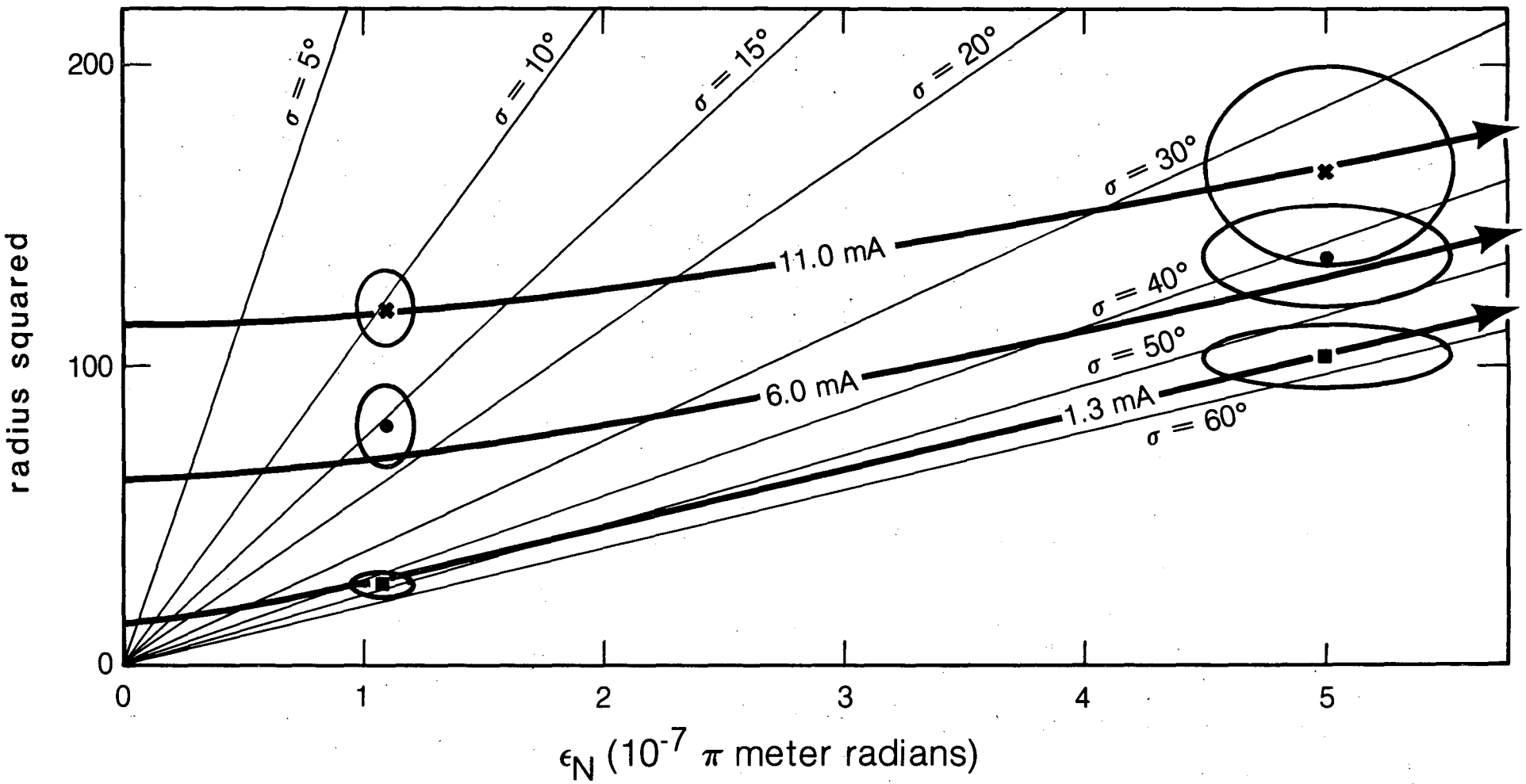

XBL 8310-592

Experimental matched beam radii (squared) for various emittances and currents in a $\sigma_0 = 60°$ lattice. Data are plotted as 90% emittances, with approximate error shown for ε. Radius measurement scatter exceeds measurement precision and is due to mismatch oscillations. Center points are average values with errors indicated as one standard deviation from mean. Currents used are ✖ 11.0 mA, ● 6.0 mA, 1.3 mA.

FIG. 2

the high-emittance points, and $\sigma = 46^\circ$, 20° and 12° for the low-emittance points. Up to two years ago -- when simulation work by Hofmann and Haber began to indicate otherwise -- it had been feared that a depressed phase advance less than 24° could not be tolerated; our measurements are important therefore in showing stable beam propagation, at least through 41 lattice periods, for σ-values well below 24°. Injector modifications planned for the near future will allow exploration of σ-values below 12°.

The most tedious part of the experimental procedure is adjusting the five matching quadrupoles, M1-M5, to obtain a matched beam. The KV envelope codes provide guidance on the initial settings of these quadrupoles but only rarely does a perfectly matched beam result from the first try. Instead, spatial oscillations of the envelope are observed and improvement in matching demands several iterations between observation and computation. For small amplitudes, the throbbing takes place about the matched beam radius, which can therefore be inferred by measurements at several locations in the transport channel. For the data in Fig. 2, the beams were matched well enough, on the average, to reduce the amplitude to about 10 percent of the radius. More sampling hardware
will be added to speed up this matching procedure.

A brief experiment was carried out for $\sigma_0 = 120^\circ$, for which a strong envelope instability for heavy space-charge loading is predicted from the KV formalism (Hofmann, Laslett, Smith and Haber, Particle Accelerators, 13, 145 (1983)). When a matched beam of 11 mA with low emittance, $1.2\times10^{-7}\pi$ rad-m, was injected into the transport channel, only 6 mA was observed to emerge from Q82, and this reduced beam was found to have a much larger emittance, $6\times10^{-7}\pi$ rad-m. Somewhat more current was, in fact, transmitted (8 mA) when the injected beam emittance was increased. Both observations are

consistent with theoretical expectations; it is intended that a more careful study be carried out in the future.

The effect of background gas collisions on the beam is through charge exchange, $Cs^+ \rightarrow Cs^\circ$ and $Cs^+ \rightarrow Cs^{+2}$. The effect on beam transmission through our 13 meter system is only about 2 percent attenuation at our lowest obtainable pressure so far (4×10^{-7} Torr).

Source Development

During the first half of the fiscal year, we developed techniques for making Cs-loaded zeolite and coating our sources uniformly with it. We installed our first "in-house" coated source in our ion gun in March. We have characterized the output of our second in-house source and found that it can sustain > 30 mA of Cs^+ emission at temperatures in the 980°C to 1000°C range, with uniformity ±10 percent, averaged across the 4 mm^2 resolution of our test stand diagnostics. The new source is equal in quality to our first one, which has shown no degradation in performance yet. The first source has already lasted four times as long as the longest-lived commercially prepared source had before its emission of Cs^+ dropped significantly.

We are also re-engineering the source heater filaments to eliminate the intrinsic heating power limitations of commercially available models. Higher source temperature is required for significantly greater emission of ions than we can presently obtain, which is desirable for future very low σ measurements, as well as for sources for future machines.

Faraday Cup Standards

In order to measure ion current, we have had to rely to date on shallow charge collectors (gridded Faraday cups) which are constrained in depth because of the need to fit between the electrostatic quadrupoles of our lattice (in a 2" gap). The large secondary electron coefficient for Cs^+ ions on solid materials in our energy range as well as ionization of desorbed gas has required us to use biased grids in front of the collector to retain the electrons, whose current is ~15 times the beam current. The grid transparency, however, is only about 98 percent, and some electrons produced from the grids can travel to the collector. We have thus had an absolute current uncertainty of about 20 percent. Even after careful study of the saturation curves of these cups, there remained an uncertainty in current calibration of some 10 percent.

We have constructed and installed a deep Faraday cup, without a grid but with a biased ring, at the exit of our channel, and have found that the current saturates ideally in both polarities (e^--retention, e^--expulsion). This cup is designed to be our standard for cross-calibration, and should provide a good absolute standard. The shallow cups have indeed shown about 10 percent less current than the deep cup indicates, and we believe that we now have a good absolute measure of ion current.

Beam Attenuation and Emittance Control

One of the major objectives of the single beam transport experiment is to explore the beam current limits in the long quadrupole-focussed channel, imposed by the beam space charge, instabilities and nonlinearities. The transport limit is measured in terms of a scaled space-charge parameter, σ (the space-charge depressed phase advance of the betatron oscillation per

lattice period). The value of σ can be varied by varying the beam current and/or the emittance as shown in Fig. 2.

Current attenuators made of fine-wire grids of various transparencies (0.035, 0.095, 0.12, 0.33, 0.39, 0.58, 0.89, 0.95, 1.00) have been mounted on an off-centered wheel in front of the source, so that the degree of attenuation can be changed by rotating the wheel without opening the vacuum system. The wheel also has several small apertures to generate pencil beams, which are useful for checking the uniformity of the source, for checking the alignment of the beam line, and for studying the coherent betatron oscillations.

The improved emittance control grids are composed of three hexcel grids (1/8" x 1/8" x 1/16" each, 0.2" thick all together). The normalized beam emittance can be varied from 1.2×10^{-7} to 6×10^{-7} π m-rad. by varying the bias voltage on the center grid from zero to 17 kV. Even with no bias voltage, the presence of the grids raises the emittance from 0.8×10^{-7} to 1.2×10^{-7} π m-rad.

BEAM DIAGNOSTICS DEVELOPMENT

Electron Beam Probe

The Electron Beam Probe (EBP) was developed as a non-destructive diagnostic of ion beam space charge. The past six months has seen two major developments in the analysis of EBP data. The first is the refinement of the model distribution described previously by replacing the uniform ion beam model with a Gaussian beam model, more nearly reflecting independent small Faraday cup measurements. The second is a new understanding of the electron halo gained with the realization that the contracting ion beam performs work on the trapped secondaries, thereby raising the electron temperature. An article by Lemons and Thode (Nucl. Fus., 21, pp. 529 (1981)) appears to supply a much needed theoretical underpinning for a detailed understanding of the mechanisms involved.

Multiple Wire Beam Profile Measurements - "HARP"

We have constructed a multi-wire beam scanner (harp) with each wire equipped with a sample-and-hold circuit coupled to a multiplexer output and then to a storage oscilloscope. Thus a profile of the beam may be taken with a single pulse.

The electrical signals on the wires arise from secondary electron emission due to ion impact. When a harp is placed between quadrupoles the neighboring positive electrodes act to draw the emitted electrons from the wires. We studied individual wires for effects on secondary emission of local electric quadrupole fields, and found that the secondary coefficient was saturated over the extent of the beam as long as at least one adjacent quadrupole was powered. Hence the current on a wire in the beam is a good

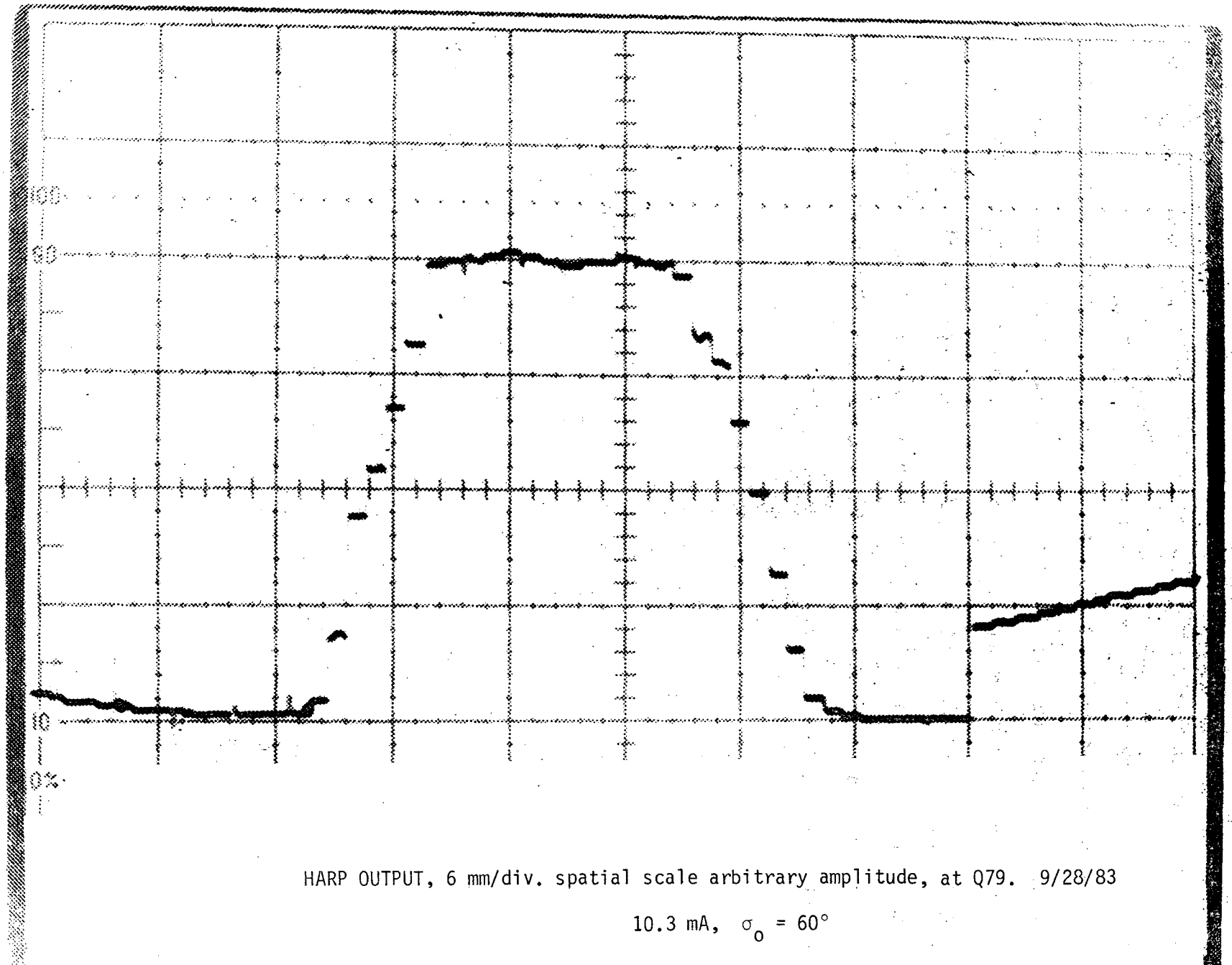

HARP OUTPUT, 6 mm/div. spatial scale arbitrary amplitude, at Q79. 9/28/83

10.3 mA, $\sigma_o = 60°$

FIG. 3

XBB 830-8932

measure of the total ion current it intercepts. Wires at a 1 mm spacing showed no significant cross-talk. A typical oscilloscope trace from the harp is shown in Fig. 3.

Several more harps are under construction, and have the capability of rotation in a plane to sample several projections. By using the reconstruction techniques that are used in the field of biomedicine (tomography, see IEEE Trans. Nucl. Sci., NS-21, 1978 (1974)), the beam distribution may be reconstructed. The same technique will allow the profiles of all the beams of a multiple beam array to be measured with a single large harp which is capable of rotation in the plane normal to the beam.

NEUTRALIZED BEAM FOCUSING EXPERIMENT

The goal of this experiment is to demonstrate focusing of a charge- and current-neutralized Cs^{+1} beam by a solenoid magnet. The major idea, due to Robertson, is that focusing occurs through the action of a beam generated collective field, in contrast to the normal situation where the magnetic force on the ion is involved. Fig. 4 gives a simplified argument concerning the lens action. In the absence of space charge forces, an electron beam passing through a solenoid would be focused relatively strongly because of its large charge to mass ratio. Correspondingly, an ion beam would be focused relatively weakly. If one had a two-component beam where the two species were strongly coupled together through space charge forces, the combined beam would come to a common focus somewhere between these two extremes. To generate the collective field to achieve the common focus, the ion beam must have sufficient current to exceed a threshold value. The large Cs^{+1} contact ionization source at LBL provides enough current density to allow a test of this idea.

In addition, the beam must be current and charge-neutralized by co-moving electrons. By placing a grid in the beam to intercept a small fraction of the ions, enough secondary electrons can be produced to neutralize the beam. A solenoid wound on the outside of the vacuum tank of the accelerator produces the magnetic field.

Major results to date include:

a. Propagation of a well neutralized intense beam over a distance of approximately 10 m (c.f. a propagation distance of 1.5 m for an unneutralized beam).

Neutralized Beam Focusing Experiment

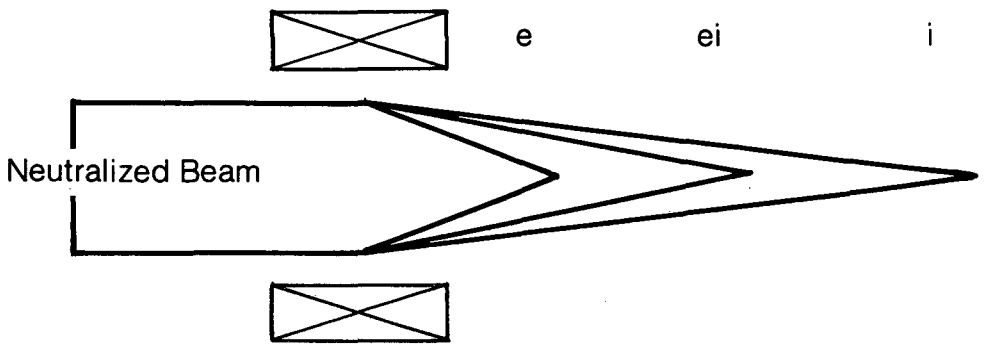

XBL 8310-590

FOCUSING STRENGTH K

$$K = \frac{1}{4}\frac{\Omega_E^2}{\nu_z^2} \quad \text{FOR ELECTRONS}$$

$$K = \frac{\Omega_I^2}{4\nu_z^2} \quad \text{FOR IONS AND GABOR LENS}$$

$$K = \frac{\Omega_E \Omega_I}{4\nu_z^2} \quad \text{FOR ROBERTSON LENS}$$

FIG. 4

b. Development of a capacitive probe which measures beam space charge potentials.

c. Determination of beam neutralization produced by the present grid configuration.

d. Discovery that the grid neutralization scheme presently in use fails to provide a sufficiently cold source of electrons for a proper test of the lens idea. Random energies of the electrons seem to be roughly of the same order of magnitude as the lens collective potential, which has the effect of washing the collective potential out, destroying the lens action.

Result number one is mainly attributable to the repair of the Cs^{+1} source hot plate. It was rebuilt and realigned, considerably improving the beam quality (as determined by envelope considerations). The beam was propagated with relatively little growth in size along the beam line. The ion current density was 0.7 mA/cm^2 at 200 kV. An unneutralized beam with equivalent current would grow due to space charge and hit the wall in about 1.5 m. This fact was demonstrated by removing the electrons with suitable biasing of the drift tubes in the accelerator.

A fast ($t_{rise} < 0.5$ μsec) potential probe was built and calibrated for use in diagnosing the beam. The main idea of the probe is to electrically isolate a capacitive pick-up from ground through a high impedance connection (operational amplifier). This means that very little charge is transferred to or from the pick-up on the time scale of a beam pulse. Consequently the pick-up disturbs the potential to be measured only by a small amount. Calibration was performed by pulsing known voltages on the drift tubes.

Using this probe one can measure the space charge potential of unneutralized beams and, more importantly, the residual potential of the neutralized beam. It was found that a residual potential of about 40 V is found at the beam edge. As the potential developed by the lens is calculated to be only 120 V, it is possible that the effect to be seen was being washed out to some extent by this residual potential. The magnetic field produced a measured collective potential, but the results do not agree with theoretical expectations in regards to size and dependence on magnetic field strength. In order to get closer correspondence with theory a cleaner experiment is needed. In particular the electron temperature should be made smaller, since in this case better neutralization is expected.

In order to get colder electrons and better neutralization, work on an annular filament cage has been initiated. Relatively cold electrons will be produced by thermionic emission from hot filaments. As the beam passes through the cage, hot electrons will be replaced by cold ones. In case the filaments do not produce enough cold electrons, an option where plasma is formed in the cage is also planned. Simulations by others indicate that a beam passing through such a cloud of electrons (or plasma) should be neutralized with residual potentials of ~1 volt. This is cold enough that the collective field of the lens should dominate the electron dynamics, an assumption of the theoretical analyses to date.

MULTIPLE BEAM EXPERIMENT (MBE)

The multiple beam experiment (MBE) is intended to test as many of the physics and engineering features of the High Temperature Experiment as are possible on a relatively small scale. The MBE will employ multiple ion-beams accelerated through a statistically interesting number of independently pulsed accelerating modules. It will serve as a test set-up to guide the most appropriate integration of the transport and accelerating components, the vacuum system, and the alignment and support structures.

Most of the ongoing activities described in this Report have a direct bearing on the definition of the MBE hardware which will be decided in the upcoming reporting period. These include physics studies with the SBTE, the insulator, module, and diagnostics developments, and the continuing conceptual design efforts on the HTE.

After discussions with K. Riepe's group (P-Division) at LANL, we have settled on 2 MeV as a suitable design goal for the pulsed injector. The injector design is proceeding at LANL; coordinating meetings between LBL and LANL staff are taking place on a regular basis.

INDUCTION ACCELERATOR DEVELOPMENT

Insulator Development

The effort in the last half year on the development of large, inexpensive insulators for accelerator applications has been in three areas: i) continuing measurements of vacuum outgassing of filled and unfilled polymers, ii) the production of Polysil® test insulators for the Naval Research Laboratory, iii) the design and specification of 5 large Polysil® insulating columns manufactured by Polytech, Redwood City, California.

The recent results in each of these areas include:

i) Vacuum Outgassing Measurements

Measurements to investigate the vacuum behavior of new composite materials have continued in cooperation with K. Riepe and E. Eaton at Los Alamos National Laboratory. During this period, we have made vacuum outgassing measurements on a filled and unfilled sample of an anhydride cured cycloaliphatic epoxy, CY-179 using hardener 907 and accelerator 065. A disc of the pure epoxy as well as one consisting of 70 percent by weight CP-01-3000 40-μm diameter glass beads were measured. Fig. 5 shows the outgassing rates as a function of time for these two samples after vacuum-baking for 24 hours at 140°C.

For comparison Fig. 6 shows the results after similar treatment of three different Polysil® formulations, which contain 85 percent by weight of silica sand and alumina powder. One of these, labeled "LBL" was made by us. The other two labeled "Polytech" were made by Polytech, Redwood City, California, and represented possible formulations to be used in the large insulating columns described under (iii).

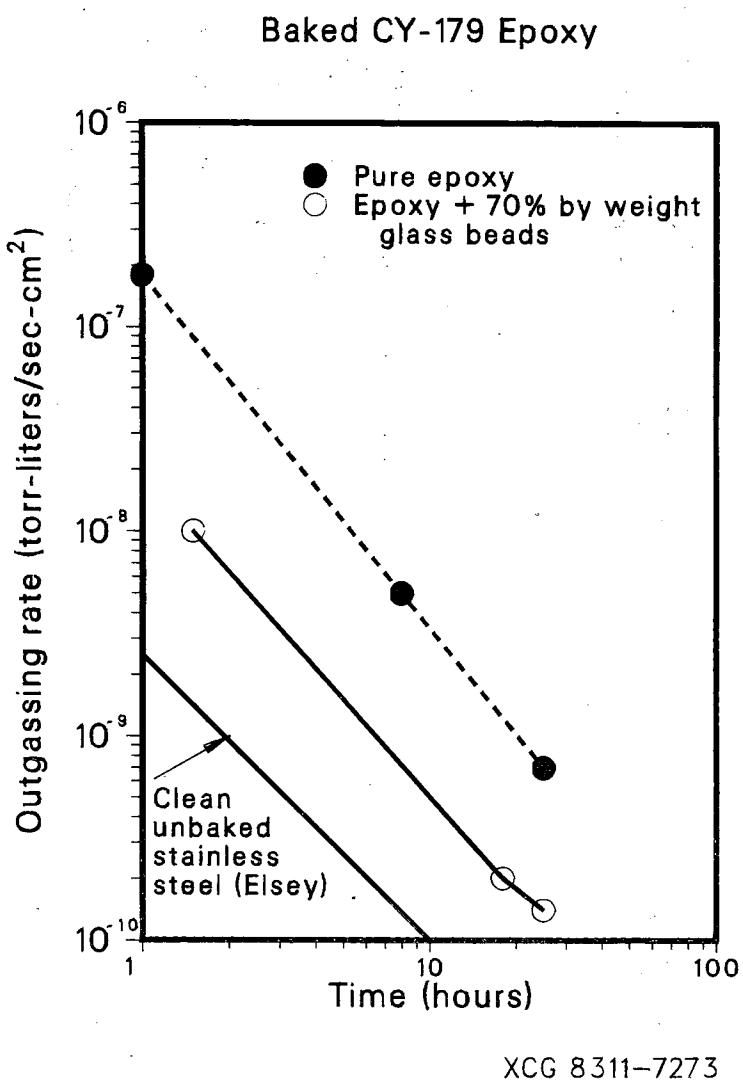
Baked CY-179 Epoxy
Pure epoxy
Epoxy + 70% by weight glass beads
Clean unbaked stainless steel (Elsey)
Outgassing rate (torr-liters/sec-cm^2)
10^{-6}
10^{-7}
10^{-8}
10^{-9}
10^{-10}
1
10
100
Time (hours)
XCG 8311-7273

FIG. 5

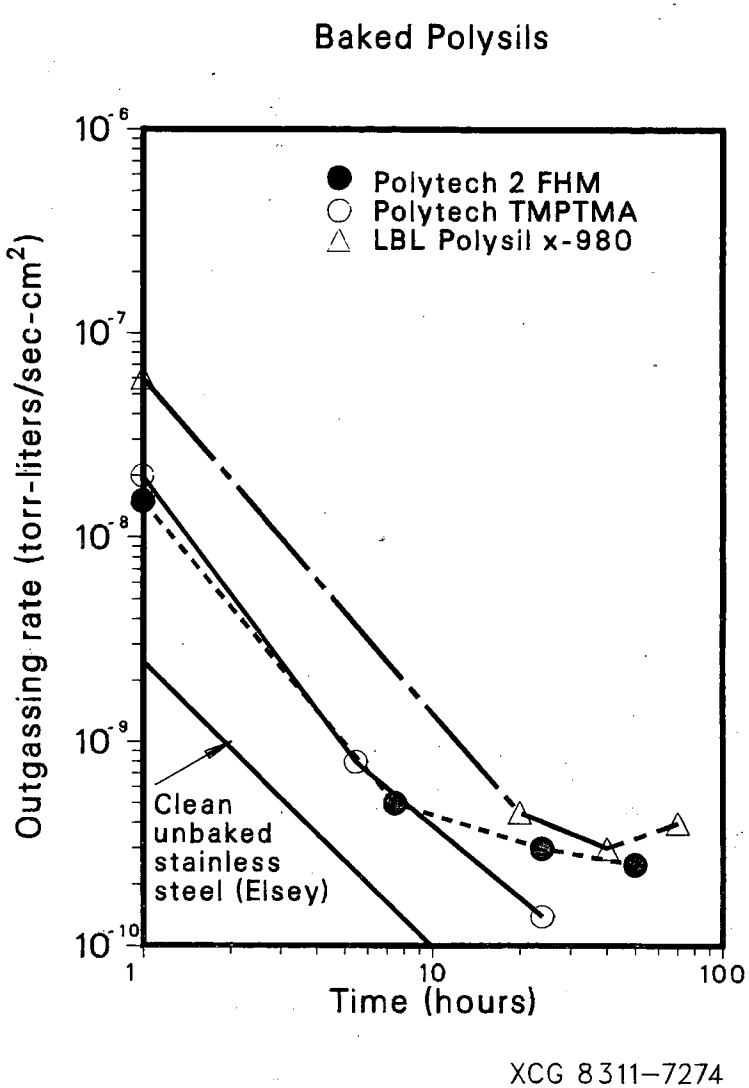
Baked Polysils
Polytech 2 FHM
Polytech TMPTMA
LBL Polysil x-980
Clean unbaked stainless steel (Elsey)
Outgassing rate (torr-liters/sec-cm^2)
10^{-6}
10^{-7}
10^{-8}
10^{-9}
10^{-10}
1
10
100
Time (hours)
XCG 8311-7274

FIG. 6

The conclusion is that the epoxy has similar behavior to Polysil® and a choice between them should be made on other grounds, e.g., material cost, ease of use, electrical behavior.

ii) The Naval Research Laboratory (NRL) program is being carried out with J. Golden and K. McDonald of NRL, who are interested in the possibility of using Polysil® for the 2-meter diameter toroidal vacuum chamber of a modified betatron. The mechanical strength and reasonable vacuum properties of Polysil® are the major attractions. The main untested question is the behavior of Polysil® under short, high voltage pulse conditions. We have fabricated a "0° Test Insulator" which will be tested at NRL in the near future. A photograph of this unit is shown in Fig. 7.

A " -45° Test Insulator" has been cast and ground to size, but has several defects which we expect to be able to patch in the next few weeks. This unit will then be sent to NRL for testing.

iii) On July 11, 1983 a contract was signed with Polytech, Redwood City, California, to produce 5 large graded insulating columns. A drawing is shown in Fig. 8.

Polytech is licensed by the Electric Power Research Institute (EPRI) to use the name Polysil® as well as the EPRI developed formulations.

These insulators will be manufactured using Polysil® formulations represented in the vacuum outgassing tests described in (i). The column size represents one that would be of interest for the High Temperature Experiment induction units. These columns have been delivered and will be vacuum tested and pulsed to high voltage to evaluate their properties in the early

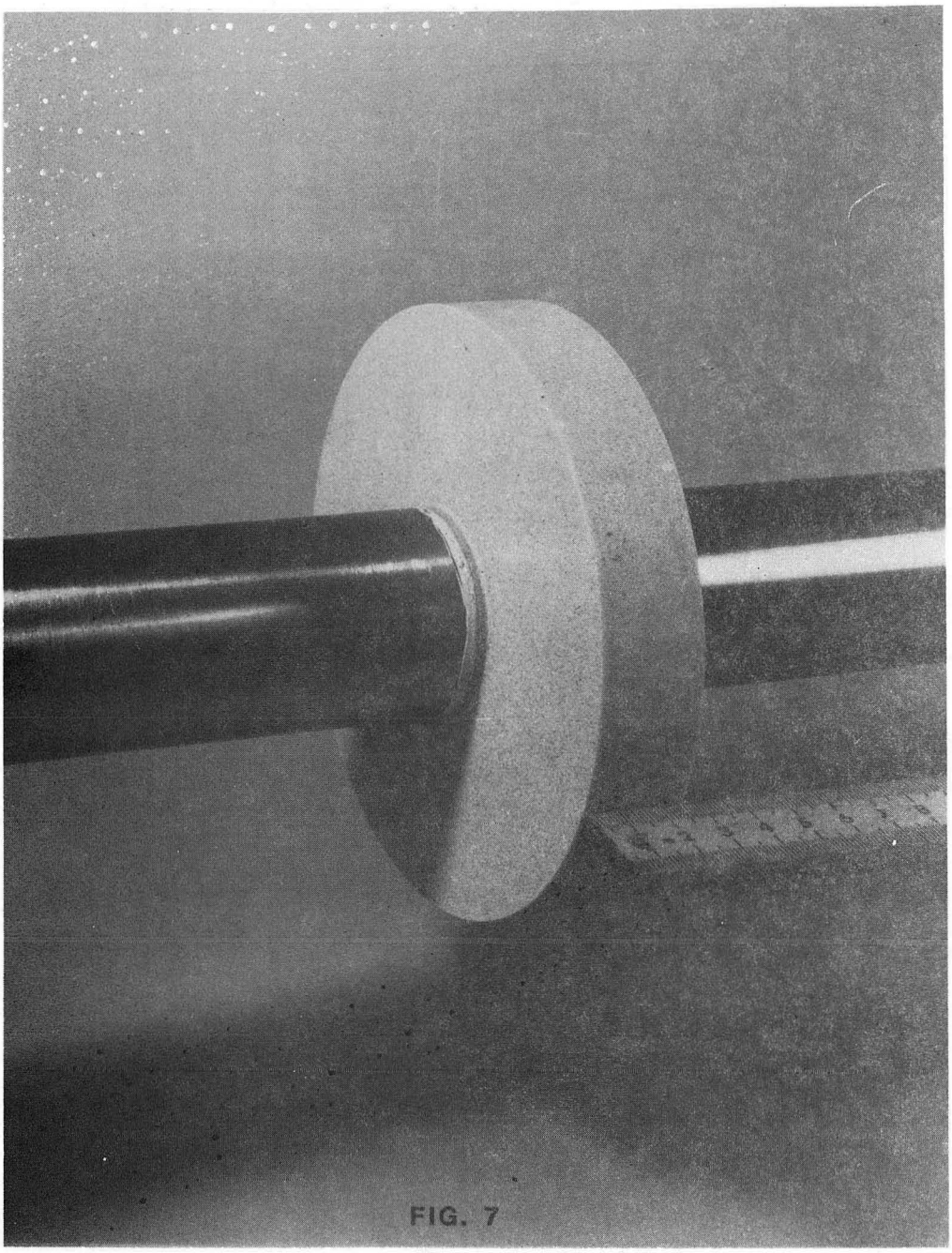

XBB 836-5071

Disk shaped Polysil® insulator on stainless steel tube (scale in cm).

Polysil Acceleration Column

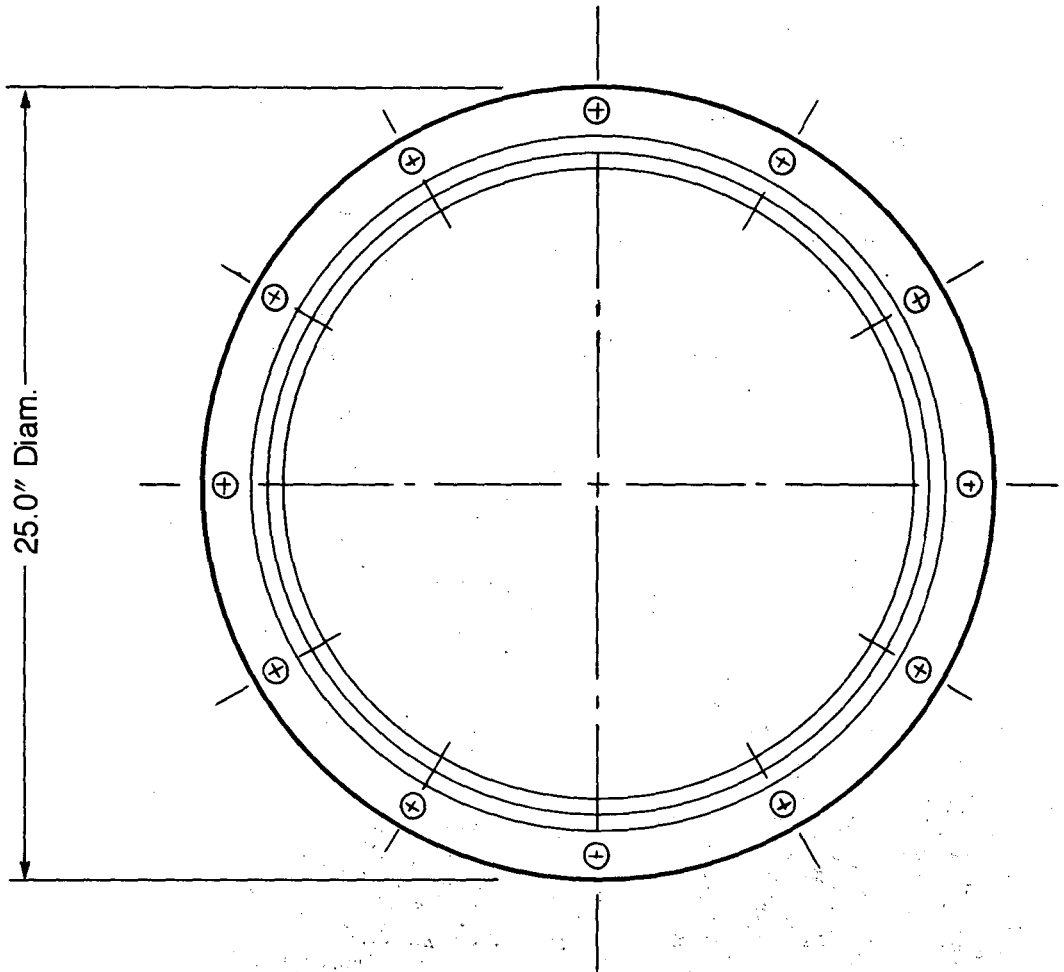

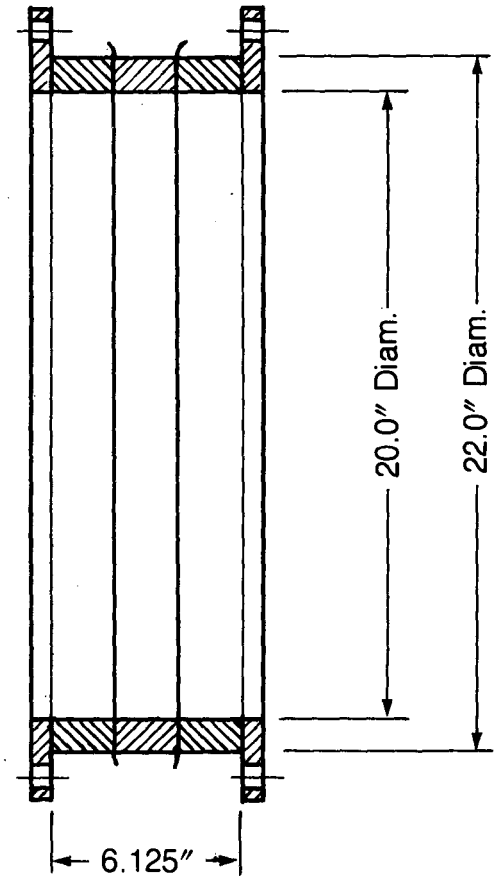

All bonded construction

FIG. 8

XBL 8310-591

part of FY 84. The cost is much less than for columns made of sintered alumina with brazed grading rings.

Long Pulse Induction Unit

During recent months the low level triggering system of the Long Pulse Induction Unit has been undergoing development to decrease time delays and variations. The initial system used SCR's or thyristors for pulse repeating and amplification purposes within the triggering chasses and in the external timing chain, and consequently the cumulative delays and jitters of three SCRs in series were added to the total delay. The variation in time delays ranged up to 1 μsec. Better SCR's and junction transistors were tried before settling on field effect transistors (FETs) for the trigger amplifiers. The FETs have negligible jitter and delay, and faster risetimes compared with the SCRs.

One long pulse module with the new triggering circuit was put on a life test which is continuing. The module at the end of September has just reached 10^6 pulses, and continues to accumulate pulses at a rate of 6×10^4 per day.

THEORY

Design of Linac for the High Temperature Experiment (HTE)

In earlier years, design and cost estimates for induction linac systems in the power-plant class (kinetic energy ~ 10 GeV, A ~ 200) were based on studies of the major portion of the linac; special regions, thought to comprise < ~20 percent of the cost, were not studied in detail. These included the linac entrance and exit regions, drift compression lines, and final lenses. For HTE systems (kinetic energy ~ 100 MeV, A ~ 20) the linac entrance and exit regions which have particular requirements nearly merge, and the drift line length is ~20-40 percent of the linac length. During FY 83 the problems of these regions have been addressed. Conceptual designs have been developed and consideration of detailed design options is under way.

A new computational framework for linac design was developed, in which bunch center position $\bar{z}$ (or acceleration $\ddot{\bar{z}}$) and bunch length ℓ are defined by given functions of <u>time</u>. Many properties of the system can then be calculated simply. These include tail-to-head velocity difference at fixed position, local charge/length and current per beam along the bunch at fixed position, required accelerating-pulse waveforms and flux changes (Volt-sec/m) at each station, and others. Transverse containment by either electric or magnetic quadrupoles is defined by occupancy factor η, low-intensity phase advance per period σ_0, and practical values of electric fields, electrode voltages, and magnetic pole-tip fields. Thus far attention has been confined to $\eta = 1/2$, $\sigma_0 = 60^\circ$, and a FODO lattice. A basic assumption is that charge/length is independent of position at fixed time.

From this information the space-charge-depressed tune σ at head and tail, cell half-length L, and maximum beam radius $\underline{a}$ can be found, subject to provision of an assumed radial clearance. Adoption of a rule for the minimum allowable σ (at the tail) leads to determination of maximum transportable charge per beam by either kind of quadrupoles as a function of z. The procedure then consists of altering the originally assumed functions $z(t)$ and $\ell(t)$ with the goals of reducing total length, attaining specified final bunch length and velocity tilt, transporting the given charge per beam, and avoiding excessive velocity tilt at intermediate positions, without requiring impractical accelerating field strengths.

By iterating this procedure, acceptable (but not fully optimized) designs have been obtained that meet a variety of requirements. They share the following properties:

1. Initial acceleration is very small until the bunch has moved by several times its length. Allowable maximum acceleration is attained only at or near the linac exit.

2. It is advantageous to use electric quadrupoles from the start (assuming 2 MeV injection) until they become too weak; they allow a shorter injected bunch and are less costly.

3. Bunch compression is not practical in the electric focusing regime; in the magnetic regime which follows, bunch length decreases at a roughly constant rate with respect to distance.

4. Within a reasonable range the velocity tilt at the linac exit may be adjusted by changes in the last 20-40 percent of the linac that have little effect elsewhere.

5. The tail-to-head velocity spread has a rather large maximum value at an intermediate distance along the linac. Imposing a prudent upper limit (~20 percent) there constrains the rate of acceleration in this region and prevents further shortening of the linac.

These results, and example designs, were presented at a DOE program review on August 30, 1983. Since then a specific reference design has been developed for more detailed study.

HTE Final Transport

The transport lines that carry the beams from the linac exit to the final lenses are extensions of the linac magnetic quadrupole arrays. Because of velocity tilt produced in the linac a drifting bunch collapses on itself longitudinally, the compression being stopped primarily by longitudinal space charge force as it arrives at the target. Ten-fold length compression and current increase are contemplated. As the current increases, σ is further depressed to very low values (of order one degree per period) at the end, and beam radius increases. To avoid excessive radial expansion higher pole-tip fields (~1 T) than those in the linac (~0.4 T, using permanent magnets) are required near the end.

Layout of these lines requires that they contain bends to aim beams at the final lenses which produce a bundle of beams converging toward the target. The maximum radius of the bundle of beams will be some meters upstream from the lens exits. This radius depends on lens system length and the convergence angle of the final bundle; the angle in turn depends on transverse size of a lens structure and on standoff distance. Based on lens design work described elsewhere in this report, this radius will be of order

3 m for the reference design mentioned above. Chromatic effects of the final bend must be controlled and are still being studied.

Line length is given roughly by the simple ballistic estimate

$$L_{line} \simeq \left[\ell_{bunch} / (\Delta p/p)_{full}\right]$$

with the right side evaluated at the linac exit. The required momentum tilt depends on final power per beam and on ion velocity and mass but not much on the compression factor. For ten-fold compression in the reference design $L_{line} \sim 200$ m and $L_{linac} \sim 500$ m. The lines are shortened by achieving more compression in the linac; the trade-off remains to be explored in detail. In this design sixteen beams are arrayed in the linac to lie along the circumference of a circle (in cross-section). Shorter linac bunches may require more beams, in a non-hollow array; the trade-off thus depends both on cost and on complexity.

HTE Design - Final Focus

The final lens system for an HTE must focus high ion currents to a radius of ~ 1.0 mm at a standoff distance of 1-2 m. It is essential that the system accommodate the predicted momentum variation of ~ ±1 percent and current variations which could be as large as ±50 percent. In addition there should be a flexibility of design that permits adjustments of spot position and accommodates a broad range of pulse energy, current and radii. A rough layout which accomplishes these aims has been realized [see Fig. 9]. It consists of four closely spaced, high field quadrupole lenses in a FDFD configuration, which are independently adjustable in strength. The beam envelope is expanded in radius through a factor of ~2.5 (by space charge)

FINAL FOCUS SYSTEM

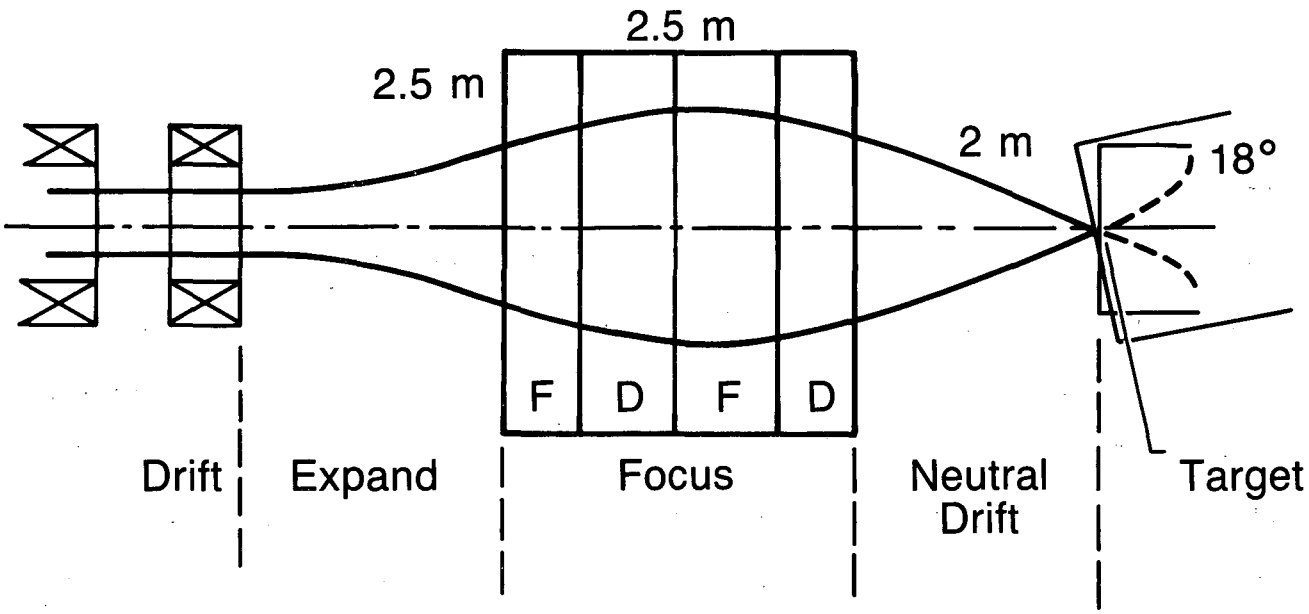

XBL 838-845A

$E = 150$ MeV (Na^+)
$I = 50$ A/Beamlet
$\epsilon_N = 4 \times 10^{-7}$ m-r/Beamlet

Spot Radius	$\leq$ 1.0 mm
Standoff	= 1-2 m
Envelope Divergence	$\leq$ 20 mr
Peak Field in Iron	< 2.0 T

FIG. 9

prior to entering the first lens. This has the effect of reducing sensitivity to space charge variations. The beam is assumed to be neutralized in transport to the target following the four lenses.

To study the properties of this focal system the coupled K-V envelope equations were solved, with initial conditions specified in the final transport system. Space charge was included and allowed to be neutralized to any assumed degree in each sector of the system. The trajectory of an off momentum particle, subject to the fields of the mean envelope was also computed.

A typical studied case (Fig. 10) is a beam of 150 MeV Na^+ ions with mean current of 50 A/beamlet and normalized emittance of 4×10^{-7} m-rad. Spot radius is dominated by momentum spread (.99 mm with ±1 percent spread or head to tail variation). Thus, there is an (expected) strong sensitivity on ΔP and it must be controlled during acceleration and compression. Current variations on the order of ±10 percent were found to be allowable if initial conditions were otherwise unchanged. A current variation of ~50 percent was found to be allowable if it was properly matched in transport (radius $\propto \sqrt{I}$). At present it is not known if this is a realistic assumption. Variations in the degree of neutrality occurring in the vicinity of the target indicate a moderate degree of sensitivity in effective spot size. While 75 percent neutrality is sufficient to achieve the desired small spot size, the standoff distance varies if this quantity is not well controlled throughout the experimental chamber. Neutralization of 90 percent or greater by electrons injected at the experimental chamber entrance is desirable, while electrons emitted from the target should be adequate for neutralization over the final 10 cm of propagation.

This preliminary study was presented at the recent HIF program review (Aug. 30). The code used to make the sensitivity calculations is QUADP,

BEAM ENVELOPE

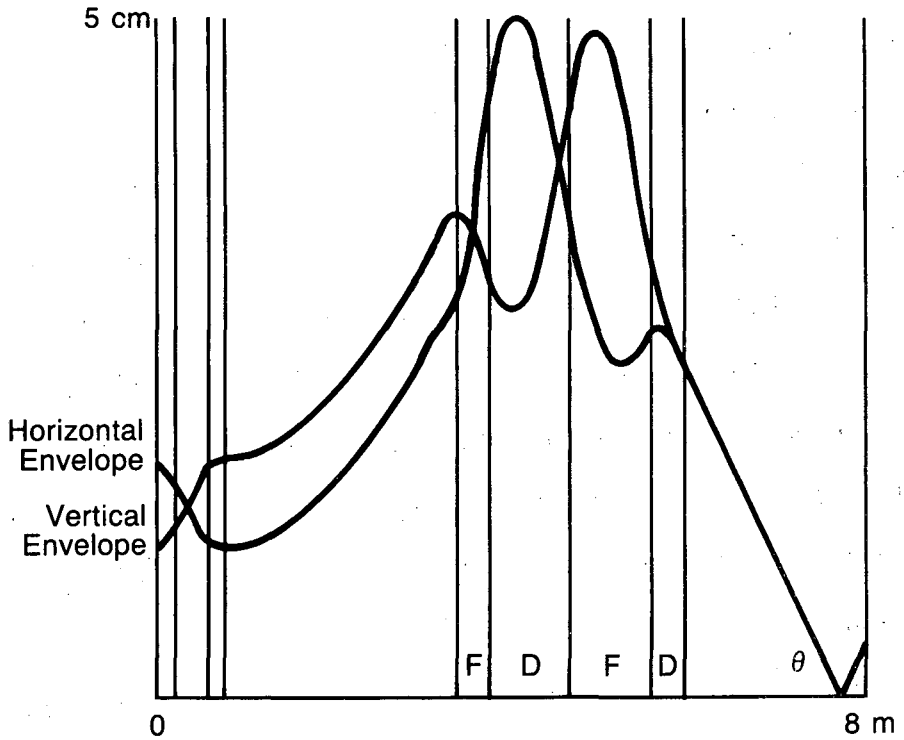

XBL 8310-3339

Spot Radius ($\Delta P = 0$)	.26 mm
($\Delta P = \pm .01$)	.99 mm
Stand Off	1.78 m
Envelope Half Angle	14.0 mr
Maximum Radius	5.0 cm
Maximum Field (Beam Edge)	1.01 T
Drift System $\sigma_0 = 60°$, $\sigma = 1.6°$	

FIG. 10

written by L.J. Laslett (LBL). It has been provided to the LANL ATD staff for further application to the final lens design.

Spot Heating Calculations for HTE

HTE will be designed to study the interaction of a high current ion beam with a material target as well test the accelerator system that produces the beam. Target temperatures in the range 50-100 eV are considered sufficiently high to examine relevant material interaction features, e.g., depositional anomalies, hot electron generation (if any), stability of the beam in a plasma plume, target charge-up, etc. Previously, the predictions for the beam-target interaction were made with the code LASNEX (at LLNL and LANL). However, this is a long-running and not generally available tool, which is not well suited for the rapid survey needed to guide HTE design. A simple model of the beam-target interaction has therefore been devised, which allows rapid approximate calculations and contains the principal physical processes revealed by LASNEX.

The target is considered to be a small cylinder of felted aluminum ($\rho \sim .05$ gm/cm^3) embedded in a hole in a lead block, which reduces expansion. Typically, the thickness of the target is double the radius and is also made equal to the ion range by felting to the appropriate density. Energy deposition is given by the beam irradiance, S, divided by the ion range, R, (evaluated at the typical plasma temperature of 75 eV). Energy loss is dominated by radiation from the front surface, which is assumed to be emitted at the instantaneous black body rate using the interior target temperature T. The rise of temperature is determined from the competition of these power flows and the equation of state function, $\varepsilon(T)$, the internal energy per gram at temperature, T. Thus,

$$\frac{d\,\varepsilon(T)}{dt} = \frac{S - \sigma T^4}{R} .$$

For felted Al at $T < 100$ eV, the dependence of specific energy is well approximated by

$$\varepsilon = 7.75\ T^{1.5}\ \rho^{-.12}\ \frac{kJ}{gm} = CT^{1.5}$$

with T given in eV and ρ in gm/cm^3.

A second phenomona which limits temperature rise is material expansion. Although the model does not directly incorporate expansion, its time scale (τ_d) is estimated to be the target depth divided by the speed of sound in the heated material. Comparison with LASNEX calculations by R. Kopp (LANL) has shown that this is a conservative measure by a factor of two, i.e., an experiment which lasts one scale expansion time does not suffer hydrodynamics degradation.

The heat equation is readily integrated to obtain $T(t)$ for given S. However, several useful scale quantities are apparent. First, there is the radiation limited temperature

$$T_f = (S/\sigma)^{1/4} \approx (56\ \text{eV})S^{1/4}$$

with S given in TW/cm^2. The time required to reach 96 percent of T_f is given by the scale cooling time

$$\tau_r = \frac{3}{2} \frac{RC}{\sigma T_f^{2.5}}$$

$$= (14.9 \text{ ns}) \left(\frac{R}{10^{-2} \text{ gm/cm}^2}\right)\left(\frac{C}{1.02 \times 10^4}\right)\left(\frac{T_f}{100\text{eV}}\right)^{-5/2}$$

To achieve the desired T_f 50–100 eV several condition must be met:

(a) Sufficient energy/gm must be applied as determined from

$$\epsilon(T_f) \approx \frac{1}{R} \int S \, dt \quad .$$

(b) This energy must be applied with pulse length shorter than or equal to the radiation scale time τ_r; hence S must be in the range of several TW/cm^2.

(c) The expansion scale time must not be short compared with the pulse length; this implies relatively deep targets.

Typical results from this model are given in Table 1.

To date, comparison with LASNEX runs (made at LANL by R. Kopp) has been made for the two cases using Na^+. The T_f value calculated here is found to lie about 15 eV above the LASNEX computed temperature and 10 eV below the peak interior temperature. For example, with 150 eV Na^+, LASNEX gives the surface temperature as 50 eV and the peak temperature as 88 eV, compared with a model prediction of (.96)(78 eV) = 75 eV.

Table 1. Predictions of Target Heating Model

Ion	E	a	I_o	S	τ_p	W	T_f	τ_r	τ_d
	MeV	cm	cm	TW	ns	kJ	eV	ns	ns
Na^+	100	.1	800	2.55	32.0	2.56	70.5	31.2	43.6
Na^+	150	.1	800	3.82	42.0	5.04	78.0	40.3	41.5
C^+	50	.1	1600	2.55	40.0	3.20	70.5	37.3	42.6
C^+	75	.1	1600	3.82	69.0	8.28	78.0	66.3	39.9

Longitudinal Stability

The theoretical understanding of high current beam dynamics typical of HIF induction linac drivers has progressed considerably during the past year. Longitudinal bunch stability, bunch compression and its impact on final focussing systems and transverse space charge limits on beam transport have been addressed both analytically and through particle simulation codes. In particular, this work has provided input for design studies of the High Temperature Experiment proposal.

Any accelerator beam is subject to longitudinal instability driven by resistive machine impedance. This resistive wall instability has been a significant factor in limiting current for a variety of accelerators. Since the induction modules of HIF drivers introduce resistive impedance which couples to the beam, it has been a major concern whether at higher currents unstable behavior would lead to unacceptable growth of longitudinal phase space.

For an infinitely long uniform density beam with no thermal velocity spread, a resistive machine impedance will yield backward moving growing waves and forward moving decaying waves. For bunched induction linac beams it has been suggested that reflection coupling of growing and decaying waves could be stabilizing. Results from a particle simulation code have confirmed this conjecture. Local growth rates which would yield several e-foldings of

growth in travelling one bunch length appear to be long term stable. From this study a threshold condition for instability has been found which determines a maximum allowable module impedance per unit length. This relation indicates that module impedances of a few hundred ohms/meter can be tolerated for a variety of single beam driver scenarios. With this limit there appears to be sufficient flexibility in machine parameters to permit both good linac efficiency and long term longitudinal stability. Work is underway to define similar criteria for multiple beams. In addition, a dispersion relation for the resistive wall instability has been derived which includes both finite transverse beam size and finite beam pipe length and radius.

Final Compression

On exiting the induction linac, the ion bunch will have a velocity tilt which will result in bunch compression during transport to the final focussing system. Any deformation of longitudinal phase space or current density during compression will affect the tolerances required of the final focussing lens system. Numerical studies of the compression have shown the importance of thermal spread in obtaining a well behaved compression.

Amplification of density perturbations during compression have been noted. This effect is reduced when modelling of the transverse variation of the longitudinal space charge force is included.

Transverse Simulation

Toward the end of the year a 2-D transverse simulation code was implemented on the MFECC Cray with computing time made available through the Office of Energy Research. Studies have begun both in support of the current beam transport experiment at LBL (SBTE) and to clarify in general the optimal

choice of tune and tune depression for the High Temperature Experiment and HIF drivers. More realistic modeling of the transverse velocity distribution have been included.

PUBLICATIONS

HI-FAN-220 LBL-15116	E.P. Lee A. Faltens L.J. Laslett L. Smith	Stablization of Longitudinal Modes in a High Current Betatron. (4/83). Presented at the 1983 Particle Accelerator Conf. Santa Fe, New Mexico, March 21-23, 1983
HI-FAN-221 LBL-15926	H.I.F. Staff	Heavy Ion Fusion Half-Year Report October 1, 1982 - March 31, 1983. (4/83).
HI-FAN-222	L.Jackson Laslett	Scaled Variables and Coefficients Describing Tune Depressions to 12 Deg. (4/83).
HI-FAN-223 LBL-16153	H. Grunder B. Leemann F. Selph	Heavy Ion Fusion with RF Linac and Cyclotron Technology (6/83) Dedicated to the Helmholtz Foundation
HI-FAN-225	W.B. Herrmannsfeldt	The New Heavy Ion Fusion Accelerator Research Program Presented at the Intern. Ion Engin. Congress Kyoto, Japan, 9/12 - 9/16, 1983
HI-FAN-226 (LBID-763)	Edward P. Lee	Spot Heating Calculation for a Heavy Ion Driven High Temperature Experiment (July 1983)
HI-FAN-227	Heavy Ion Fusion Staff, Los Alamos National Laboratory Lawrence Berkeley Laboratory (Compiled by R.O. Bangerter)	Heavy Ion Fusion Accelerator Research Program Plan for FY84-FY-89. (8/83)
HI-FAN-228	Joseph J. Bisognano	Comments on the Longitudinal Stability of Induction Linac Bunches for HIF. (9/83)
HI-FAN-229	L. Jackson Laslett	H.-T.-E. Induction Linac. (10/83)
HI-FAN-230 LBL-16639	A. Faltens D. Keefe	Power-Amplification of a Heavy-Ion Beam In An Induction Linac. (10/83)

HEAVY ION FUSION ROSTER

Denis Keefe

Clarence Chavis
Warren W. Chupp
Edwin R. Edwards
Andris Faltens
Milton Firth
Edward C. Hartwig
Charles H. Kim
Michael Lampel
Edward J. Lofgren
Chester D. Pike
Stephen S. Rosenblum
Gerald L. Stoker
Michael Tiefenback
David Vanecek
Anthony Warwick

Lloyd Smith

Joseph Bisognano
Victor Brady
D. L. Judd
Geoffrey Krafft
L. Jackson Laslett

William B. Herrmannsfeldt, SLAC

HALF-YEAR REPORTS: Distribution List

Argonne National Lab.

Thomas A. Fields
Ronald Martin

University of Arizona

R. Morse

Batelle

John Hartman

Bechtel

W. Allen

Brookhaven National Lab.

Mark Barton
Alfred Maschke

C.E.A. Bruyeres-le-Chatel

R. Dei-Cas

University of Calif., Irvine

Norman Rostoker

University of Calif., Riverside

Robert Poe

Cornell University

John Nation
Ravi N. Sudan

DARPA

Richard Gullickson
Joe Mangano

Department of Energy

DP

S. Barish
Sheldon L. Kahalas
L. Killion
H. Roser, Asst. Sec., Defense Programs
R. Schriever

ER

Terry Godlove
James S. Kane
Richard Kropschot
James Leiss
Gerry Peters
David F. Sutter
Alvin Trivelpiece, Dir., Office of Energy Research
William Wallenmeyer

DoE San Office

Rudolf Bredderman
Z. Zafiris

E.P.R.I.

Ken Billman

Fermi National Accelerator Lab.

Frank T. Cole
Fred Mills
Lee Teng

GANIL

P. Lapostolle

GSI

R. Bock
D. Boehne
Ingo Hofmann

University of Illinois

G. Miley
Joseph Verdeyen

KMS Fusion, Inc.

Alex Glass
Henry J. Gomberg

Kanazawa University

S. Kawasaki

Lawrence Berkeley Laboratory

Bob Avery
Joseph Bisognano
Warren Chupp
Tom Elioff, 46C
Andy Faltens
Al Garren
Hermann Grunder, 50/149
Ed Hartwig
Egon Hoyer
Earl Hyde, 50A/4133E
Rob Johnson, 50/149
Dave Judd
Denis Keefe
Charles Kim
John Knight, 62/203
Martha Krebs, 50A/4112
Wulf Kunkel, 4/230
Glen Lambertson
L. Jackson Laslett
Ed Lee
Edward Lofgren
Jack Peterson
Stephen Rosenblum
Andrew Sessler, 4/230
Bill Shanahan, 50C/001
David Shirley, 50A/4113
Lloyd Smith

Lawrence Livermore Laboratory

Richard J. Briggs, L-321
John L. Emmett, L-488
John Holzrichter, L-481
William Krupke, L-488
Jim Mark, L-477
Michael J. Monsler, L-481
John Nuckolls, L-477

Lockheed

John Siambis

Los Alamos National Laboratory

Roger Bangerter
Ihor Bohachevsky
Richard Cooper
Robert Jameson
Don Kerr
A. Peaslee
Roger B. Perkins
Steve Rockwood
George Sawyer
Sid Singer
Richard Stokes
Don Swenson
Tom Wangler

University of Maryland

Martin Reiser
Derek Tidman

Maxwell Laboratories

Library

National Bureau of Standards

S. Penner
M. Wilson

National Science Foundation

Edward Knapp, Director

Naval Research Lab.

Steven Bodner
T. Coffey
Irving Haber
Philip Sprangle
Peter Turchi

Occidental Research Corp.

Wyn Salisbury

Physics International

Library

RAFAEL

Joseph Shiloh

Rutherford Laboratory

John D. Lawson
Chris Pryor

Sandia Laboratories

Everet H. Beckner
Don Cook
Tom Martin
J.P. Vandevender
Gerold Yonas
Glenn Kuswa

Soka University

Tetsuya Saito

SOREQ Nuclear Research Center

A. Sternlieb

SLAC

William Herrmannsfeldt
W. K. H. Panofsky
Burton Richter

TRW

J. Gordon
Z. Guiragossian
J. Maniscalco

Westinghouse

E. W. Sucov

University of Wisconsin

G. Kulcinski
G. Moses
R. Peterson

This report was done with support from the Department of Energy. Any conclusions or opinions expressed in this report represent solely those of the author(s) and not necessarily those of The Regents of the University of California, the Lawrence Berkeley Laboratory or the Department of Energy.

Reference to a company or product name does not imply approval or recommendation of the product by the University of California or the U.S. Department of Energy to the exclusion of others that may be suitable.

TECHNICAL INFORMATION DEPARTMENT
LAWRENCE BERKELEY LABORATORY
UNIVERSITY OF CALIFORNIA
BERKELEY, CALIFORNIA 94720